



## Effects of Brace-viscous Damper System on the Dynamic Response of Steel Frames

A. Pourzangbar\*<sup>a</sup>, M. Vaezi<sup>b</sup>, S. M. Mousavi<sup>c</sup>, A. Saber<sup>a</sup>

<sup>a</sup> Dipartimento di Ingegneria, Civile, Edile e di Architettura, Università Politecnica delle Marche, Italy

<sup>b</sup> Department of maritime engineering, Amirkabir University of Technology, Tehran, Iran

<sup>c</sup> Department of Civil Engineering, National Taiwan University, Taipei, Taiwan (R.O.C)

### P A P E R I N F O

#### Paper history:

Received 04 November 2019

Received in revised form 18 February 2020

Accepted 07 March 2020

#### Keywords:

Brace-viscous Damper System

Damper Configuration

Tabas Earthquake

ANSYS

Dynamic Response

### A B S T R A C T

In this study, the effects of three different viscous damper configurations, chevron, diagonal and toggle, as well as brace stiffness on the performance of brace-viscous damper system in various steel frames under different earthquake records were investigated. A finite element software, ANSYS, is exploited to develop the numerical models. To verify the numerical simulations, their results were compared with those of the experimental studies in the literature. The results show the reduction in the base shear force given by the toggle configuration is larger than that due to the chevron and diagonal configurations. Regarding the brace stiffness (area), for a reference damping coefficient of 500 N.m/s, a 54% increase in the brace area (from 42 to 91.8 mm<sup>2</sup>) results in a 21.26, 38.61, and 17.57% reduction in the structure displacement response for the diagonal, chevron, and toggle configurations, respectively. Further, using the results of the numerical simulations, we proposed the spatially-optimized distribution of the brace-viscous damper system.

doi: 10.5829/ije.2020.33.05b.02

## 1. INTRODUCTION

When the structures are exposed to the effects of dynamic loads such as an earthquake, the energy from this natural phenomenon is transferred to the structure, and as a result of this, the structure begins to vibrate in various modes. Vibration lasts as long as the transferred energy to the structure is completely dissipated. In structures without energy dissipation equipment, the dissipation of energy in the elastic range is very small and the majority of energy dissipates through the friction in the joints. If the intensity of these loads is high, large displacements will happen in the structure. In this case, the structure maintains its stability due to the changes in non-elastic displacements. Such large displacements create plastic joints at different points of the structure which result in increased ductility and energy depletion. In this case, a large amount of energy is lost due to local degradation. There are two solutions to counteract the formation of plastic joints in concrete and steel structures: 1) increasing the stiffness of the structural parts, which is not economical for large structures, and 2) using the

energy dissipation tools also known as the control systems such as dampers, which prevent the vibration phenomenon due to their specific performance. Today, the application of the control systems is very common in order to prevent vibrations of structures against seismic loads. Structural control technologies have achieved remarkable success in reducing the vibrations of structures rooting in dynamic loads such as wind force, earthquake, and ocean waves [1–6].

Generally, energy dissipation (or control) systems are classified into four types including (1) passive (inactive) control systems, with high energy dissipation density and no need of an external power source; (2) active control systems, with force delivery devices and real-time processing sensors that need power for the actuator to generate a structural control force; and (3) semi-active control systems, that change some structural parameters while consuming less power compared with active control systems and (4) hybrid control systems [7–9]. Since the viscous dampers are commonly used among passive control systems for energy depreciation, in this paper we only discuss these systems.

\*Corresponding Author Institutional Email:  
A.pourzangbar@pm.univpm.it (A. Pourzangbar)

For many years, passive dampers have been widely used at low cost and minimum maintenance requirements to reduce the dynamic response of structures, and significant progress has been made regarding the use of various dampers in different structures. Ou et al. [10] investigated the seismic response of structures with velocity-dependent passive energy dissipation devices with special attention on the brace-viscous damper control systems. Their results verified the effectiveness of the passive energy dissipation devices for the suppression of dynamic responses of structures. Yu et al. [11] determined a robust optimal framework for tuned mass damper (TMD). Their numerical simulations demonstrate that their developed framework is a powerful tool for the optimal design of the TMD and also improves in the efficiency of the TMD performance.

Constantinou and Symans [12] conducted an experimental study of the seismic response of buildings with supplemental fluid damping devices. The experimental results suggest that the use of viscous dampers to the tested steel structure model resulted in the reductions of inter-story drifts, floor accelerations and story shear forces by factors of two to three in comparison with the response of the same structure without the dampers. Hwang et al. [13] studied the feasibility of implementing seismic protective systems into high-tech industrial structures in which costly vibration-sensitive facilities are housed. Their simulation results showed that the proposed control scheme is effective to suppress the vibration of the high-tech industrial structures. Tabeshpour and Komachi [14] discussed the importance of retrofitting offshore jacket platforms under extreme loads. They talked in detail how to use friction damper device and buckling restrained braces can reduce structural responses and increasing seismic performance level of the offshore jacket platforms. Despite they have been commonly used in different structures, less can be found in literature to compare the chevron, diagonal and toggle damper configurations effects on the structure response to the dynamic loads which is the focus of this research. Although the above-mentioned studies proved the efficiency of the viscous damper in the mitigation of structures' dynamic response, the implementation of the viscous damper systems with various dampers' configurations has led to most optimal designs.

McNamara et al. [15] implemented the toggle brace damper (TBD) system to a 39-story office building located in Boston (U.S.A.). Their results indicated that the stiffness of the toggle braces is very important for increasing the effectiveness of the overall damping system. Zhang et al. [16] studied the effects of toggle-brace-damper installation modes on stiff structures. They suggest that the upper toggle-brace-damper system has the largest magnification factor, which is consistent with the theoretical analyses. The brace deformation and

installation error cannot be ignored in the design of a toggle-brace-damper system. Installation error can also lead to out-of-plane instability of a toggle-brace-damper system. Moreover, the experimental results show that the magnification factor changes with loading and is different when force is applied in the push and pull directions. In another study, passive vibration control of a mosque structure under two types of damping systems, say diagonal bracing damper and toggle bracing damper, have been analyzed [17]. This shows that the damping coefficient in the toggle bracing damper configuration is smaller than the diagonal one.

Brace stiffness and configurations have also been a focus of interest in several research studies. Chen and Chai [18] discussed the effects of brace stiffness on the performance of structures with Maxwell model-based brace-damper systems. The effects of brace stiffness on the overall performance of the building are quantified in their results. Dethariya and Shah [19] studied the effects of viscous dampers on the dynamic response of a 9-story structure. They investigated the various configurations of the dampers and showed that dampers configuration is directly proportional to the structure response mitigation. Sarno and Elnashai [19] investigated the seismic performance of steel structures retrofitted with three structural configurations: special concentrically braces (SCBFs), buckling-restrained braces (BRBFs) and mega-braces (MBFs). They could conclude that maximum story drifts of MBFs are lower than MRFs and SCBFs. Türker and Bayraktar [20] also studied experimentally and numerically the brace configuration effects on steel structures. Among the all, they chose cross-type,  $\Lambda$  type, V type and K type brace configurations. Their finite element models in SAP2000 along with their experimental results show that the effects of braces vary depending on brace configurations.

Regarding the above mentioned statements, although viscous dampers could reduce the structure response significantly, the classic approaches in utilizing the viscous dampers may render them ineffective. For example, using common K-shape and diagonal braces with viscous dampers for shear wall structures and high-rise buildings are not effective and may increase costs [21]. The proper design of control tools is costly; however, it will increase the structural efficiency by adjusting the dynamic parameters such as the configuration of viscous dampers or brace stiffness. To improve the performance of the control systems, it is recommended to apply different configurations to the brace-viscous damper systems. Moreover, an increase in the amount of braces stiffness attached to the damper may affect positively on the mitigation of the structure response.

Although several studies have dealt with the effects of viscous dampers and braces on the mitigation of the dynamic response of the various structures such as inland

and marine structures [22–24], there is a gap in conducting a study that simultaneously investigates all the effects of viscous dampers' configurations (i.e. chevron, toggle, and diagonal) and distributions (i.e. uniform or non-uniform), as well as brace stiffness, on the dynamic response mitigation of steel frame structures. Therefore, the main aim of this contribution is developing an efficient brace-viscous damper system could be of great importance in the reduction of the costs and increase of the stability of the structure.

This paper is structured as follows: The effects of various configurations of viscous dampers as well as brace stiffness on the performance of the brace-viscous damper systems in the reduction of dynamic response are presented in Section 2. The modelling approach and the data on the basis of the analyses are given in Section 3, which is followed by the results and discussion of Section 4. Finally, Section 5 (conclusions) closes the paper.

## 2. BRACE-VISCOUS DAMPER SYSTEM

**2. 1. Viscous Dampers** Viscous dampers mitigate the dynamic energy transferred to the structure via the movement of the piston through a highly viscous fluid, and the damping force is out-of-phase with the viscous damper deformation [12]. Viscous dampers are the ones in which the produced resilient force is directly proportional to their axial displacement velocity. The behavior of viscous dampers is described by Equation (1) [25]:

$$F_D(t) = C_D |\dot{U}(t)|^N \text{sgn}(\dot{U}(t)) \quad (1)$$

where  $F_D(t)$  is the force generated by the damper,  $C_D$  is the damping coefficient,  $N$  is a constant depending on the damper shape and ranging from 0.3 to 1.95,  $\dot{U}(t)$  is the axial velocity of the damper piston,  $t$  is time, and  $\text{sgn}(\cdot)$  is the sign function.

According to Equation (1), the resistant forces of viscous dampers are directly proportional to their axial velocity (Equation (2)), which depends on their amplitude of displacement [12]. Therefore, the damping force of viscous damper, which is a criterion for evaluating their performance, depends on their axial velocity (Equation (2)):

$$\dot{U}(t) = A_0 \frac{2\pi}{T} \cos\left(\frac{2\pi}{T}t\right) \quad (2)$$

where  $T$  is the period of the damper displacement, and  $A_0$  is the amplitude of the damper displacement. Referring to Equations (1 and 2), an increase in  $\dot{U}(t)$  will increase  $F_D(t)$  until  $F_D(t)$  reaches to its maximum value. In viscous dampers implemented in inland structures,  $\dot{U}(t)$  is not so large to produce the maximum  $F_D(t)$  because the interaction between the viscous damper, brace and structure decreases the  $\dot{U}(t)$ . The most efficient

performance of a brace-viscous damper system is achieved when the viscous damper axial velocity ( $\dot{U}(t)$ ) has its maximum value. The viscous damper configuration as well as brace stiffness are among the governing parameters can produce the most efficient brace-viscous damper system.

## 2. 2. Performance of Brace-Viscous Damper System

The performance of viscous dampers are affected by (1) the resistant forces of viscous dampers ( $F_D(t)$ ) which directly is proportional to the axial velocity of the viscous damper, and (2) their damping ratio ( $\beta$ ) which means how oscillations in a system decay after a disturbance.

The relation between the horizontal component of the force exerted by the viscous damper on the frame in which the damper is connected ( $F_h(t)$ ) with the resistant forces of viscous dampers ( $F_D(t)$ ) can be represented using Equation (3):

$$F_h(t) = f F_D(t) \quad (3)$$

where  $f$  is the displacement magnification. The  $F_h(t)$  is larger than  $F_D(t)$  in the case of chevron configuration while it is less than  $F_D(t)$  in the case of diagonal configuration [12]. Considering Equation (2), it can be concluded that increasing the displacement magnification ( $f$ ) leads to the large resistant forces of the viscous damper ( $F_D(t)$ ) and consequently large exerted forces to the frame ( $F_h(t)$ ). The latter finding is indicative of the improvement in the performance of the viscous damper. Further, according to the FEMA [26], the damping ratio produced by viscous dampers in  $k^{th}$  vibrational modes ( $\beta_K$ ) is calculated using Equation (4):

$$\beta_K = \frac{T_K \sum_j C_j f_j^2 \phi_{rj}^2 g}{4\pi \sum W_i \phi_i^2} \quad (4)$$

where  $T_K$  is the vibration period in mode  $M$ ,  $\phi_i$  is the displacement of  $k^{th}$  mode on the floor ( $i$ ),  $\phi_{rj}$  is the relative displacement of the  $k^{th}$  mode on the floor ( $j$ ),  $C_j$  is the damping coefficient of the damper installed on the floor ( $j$ ),  $f_j$  is the system magnification coefficient, including the damping device coefficient ( $C_j$ ),  $W_i$  is the effective weight of the floor ( $i$ ).

According to Equation (4), there is a direct relationship between the damping ratio ( $\beta$ ) and the second power of the displacement magnification ( $f$ ). Furthermore, it demonstrates that the configurations with  $f \geq 1$  are very efficient in producing large values of damping ratio ( $\beta$ ) even with low values of damping coefficients. Using the proper configurations for the viscous dampers, the coefficient of the displacement can be increased. Therefore, the damper configuration can play an important role in the mitigation of the displacements. In order to study the effects of viscous dampers configurations, three well-known

configurations, i.e. chevron, diagonal and toggle configurations, is discussed in the current contribution.

**2. 2. 1. Diagonal, Chevron and Toggle Configurations**

Viscous damper used in structures has a specific range of axial displacement amplitude. During the vibration of the structure, if the axial displacement amplitude of the damper (and consequently its axial velocity) reaches its maximum limit, the damper’s functionality would be improved and so it utilizes its maximum capacity to produce resistant force. Otherwise, the full capacity of the damper will not be used. With the proper configuration of the damper in the structure, its resistant force ( $F_D(t)$ ) and consequently, the damper’s functionality can be improved. There are three types of damper configurations, i.e. diagonal, chevron and toggle configurations.

As shown in Figure 1A, in a diagonal configuration, the damper is located along the brace axis ( $C_D$  is the damping coefficient). The axial displacement magnification in this configuration is  $f = \cos \theta$  in which  $\theta$  is referred to the slope between the viscous damper and horizontal axis (Figure 1A). In this configuration,  $\theta$  is always between  $0^\circ - 90^\circ$ , and  $f$  varies in the range of  $0 - 1$ .

The chevron damper is installed in the upper section of the braces and parallel to the story level. The inclination of the damper in the chevron configuration is zero. The magnification coefficient of the displacement in this configuration is one [12]. In other words, the axial displacement of the damper equals the story drift (Figure 1B). According to Equation (4), the damping ratio has a direct relationship with the magnification coefficient of the damper, so the produced damping ratio associated with the chevron configuration is larger than that of the diagonal configuration.

In the toggle brace system, the damper is installed diagonally from its first end-jointed to the beam-column connection and its other end to the brace connection (Figure 1C). In this case, the magnification factor depends on the angles of both braces and damper ( $\theta_1, \theta_2$  and  $\theta_3$ ). For the chevron configuration  $f = 1.0$ , while for the diagonal configuration  $f = \cos \theta$  (where  $\theta$  is the inclination of the damper) [12]. The magnification factor is then obtained by Equation (5), as suggested by Zhang et al. [27]:

$$f = \frac{\sin \theta_2}{\cos(\theta_1 + \theta_2)} \cos(\theta_3 - \theta_1) + \sin \theta_3 \tag{5}$$

Equation (5) reveals that the magnification factor attains very large values as  $\theta_1 + \theta_2 \rightarrow 90^\circ$ .

In the toggle configuration, the magnification coefficient can be greater than one. According to Equation (4), the produced damping ratio due to toggle configuration may be several times larger than that of the chevron and diagonal configurations. For instance,

assume a damper with a constant damping coefficient ( $C_D$ ) but three different configurations (chevron, toggle and diagonal). If the damping ratio ( $\beta$  in Equation (4)) associated with the diagonal configuration (when  $\theta = 45^\circ$ ) is 3%, the damping ratio for chevron and toggle configurations are 4.7 and 30-42.3%, respectively.

As a result, it is possible to produce large forces using suitable dampers’ configurations and small damping coefficients, which leads to more control in the seismic response of the structures. Due to a large amount of magnification coefficient in the toggle configuration, this configuration can be used to control vibrations in hard structures with low lateral displacements (such as concrete structures with shear walls) or structures exposed to wind forces.

**2. 2. 2. Brace Stiffness Effects on the Performance of Brace-Viscous Damper System**

The shear forces of the stories result from the difference in the axial displacements of the damper and the story, has a negative impact on the performances of the damper. In other words, we are seeking to find a brace-viscous damper system in which the displacements are similar to the story drifts and there are no excessive shear forces. This aim could be achieved by setting proper values for the brace stiffness. According to the complex damping theory [10], the loss factor ( $\eta_{vb}$ ), the energy dissipation capacity of a brace-viscous damper system can be calculated using Equation (6):

$$\eta_{vb} = \frac{K_{vb}''}{K_{vb}'} = \frac{K_b}{C_D \omega_0} \tag{6}$$

where  $K_{vb}''$  is the energy dissipation capacity of the damper-brace component;  $K_{vb}'$  expresses the additional stiffness of the structure due to the combination with the brace-damper system;  $K_b$  is the axial stiffness of the braces;  $C_D$  is the damping coefficient of the viscous damper and  $\omega_0$  is the natural frequency of the structure.

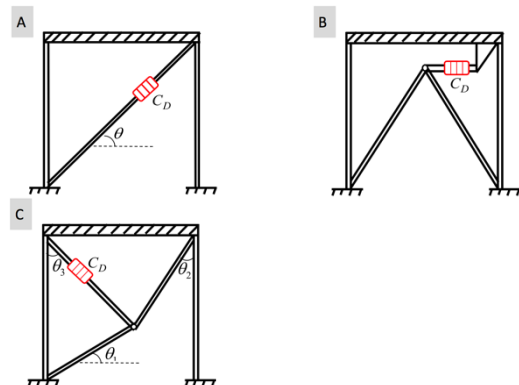


**Figure 1.** The various configurations of a viscous damper; (A) Diagonal configuration [13], (B) Chevron configuration [13], (C) Upper Toggle Brace Damper (UTBD) configuration [12]

The ratio  $K''_{vb}/K'_{vb}$  indicates the ability of brace-viscous damper system in dissipating the dynamic energy. When this ratio is one (which is achieved using very larger values of  $K_b$ ), the system reaches to the highest value of its energy dissipation capacity and will have the most suitable performance. As expressed, the brace stiffness can control the energy dissipation capacity of brace-viscous damper system.

### 3. NUMERICAL MODELLING APPROACH

#### 3. 1. Case Study and Dynamic Loading

The effect of viscous dampers' configuration and braces' stiffness on the brace-viscous damper system performance is studied using four earthquake acceleration records including the Tabas, Northridge, EL-Centro and Kobe earthquake records (Figure 2). The Tabas earthquake took place on Saturday 16 September 1978 at 19:38 local time when the majority of people were at home [28]. The shock was a large magnitude earthquake with 7.4 on the moment magnitude scale and had a maximum Mercalli intensity of IX+ (Violent) and at a shallow depth of approximately about nine kilometers. The death toll was in the range of 15,000–25,000 with severe effects in the town of Tabas. The 1940 El Centro earthquake (or 1940 Imperial Valley earthquake) occurred at 21:35 Pacific Standard Time on May 18 (05:35 UTC on May 19) in the Imperial Valley in south-eastern California near the inter-national border of the United States and Mexico. The Great Hanshin Earthquake, or Kobe earthquake, occurred on January 17, 1995 at 05:46:53 JST in the southern part of Hyōgo Prefecture, Japan, including the region known as Hanshin. It measured 6.9 on the moment magnitude scale and had a maximum intensity of 7 on the JMA Seismic Intensity Scale. The 1994 Northridge earthquake was a moment magnitude 6.7 (Mw), blind thrust earthquake that occurred on January 17, 1994, at 4:30:55 a.m. PST in San Fernando Valley region of the County of Los Angeles. Its epicentre was in Reseda, a neighbourhood in the north-central area of the San Fernando Valley.

In order to understand the effects of dampers' configuration and also braces' stiffness, three different types of viscous dampers including diagonal, chevron, and toggle configurations have been installed in the reference structure (e.g. Figure 3 shows the properties of braces and dampers in the four-story frame). Three steel frames, including a 3-story, a 6-story, and a 9-story steel structure, have been considered to develop the numerical simulations. Figure 4 indicates the 3-dimensional view of the structures with the diagonal configuration. Figure 5 shows the results of these structures design for only some selected frames. We used the AISC 360-10 manual to design these steel structures.

The structure has four stories with a steel frame. Table 1 summarizes the information of the braces and columns.

Regarding the identity of applied loads (Tabas earthquake mapping acceleration record), the transient time history analysis has been utilized. To understand the effects of braces' stiffness (braces' area), the different areas for the braces have been used as indicated in Table 2. As indicated, 12 different states for braces' area are

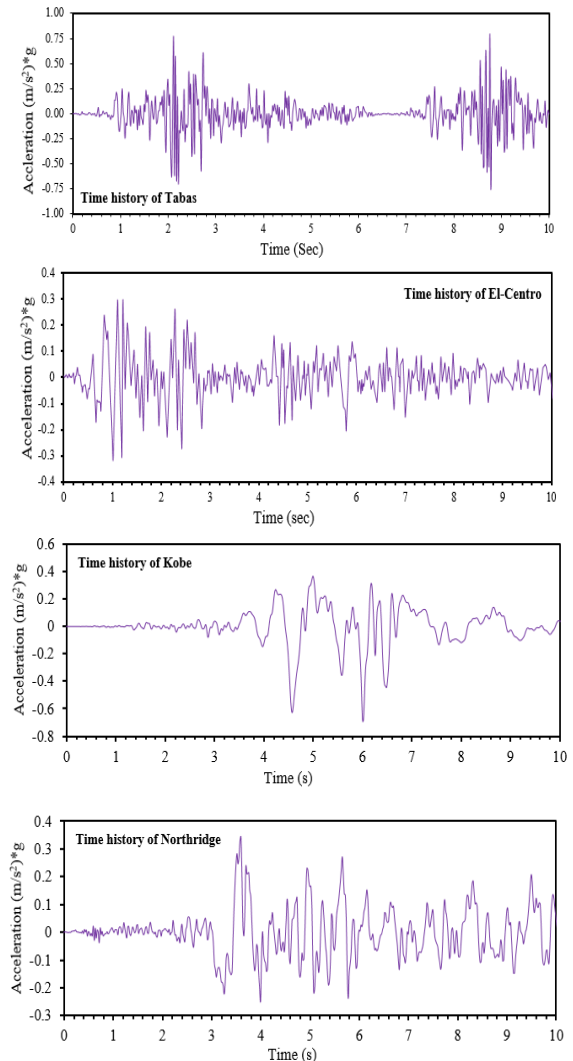


Figure 2. Time history of the acceleration records for the earthquakes considered in the current paper

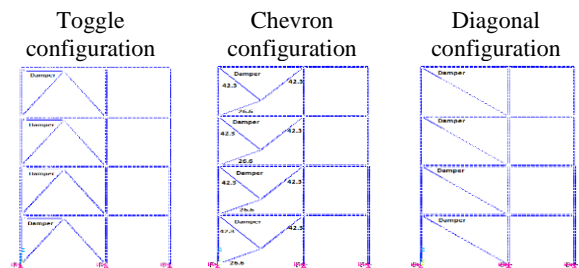
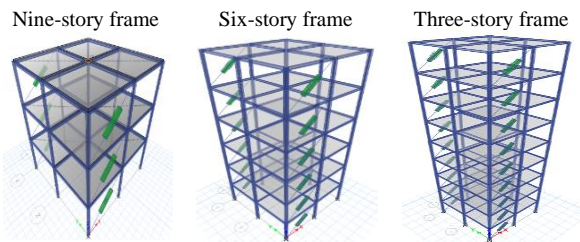
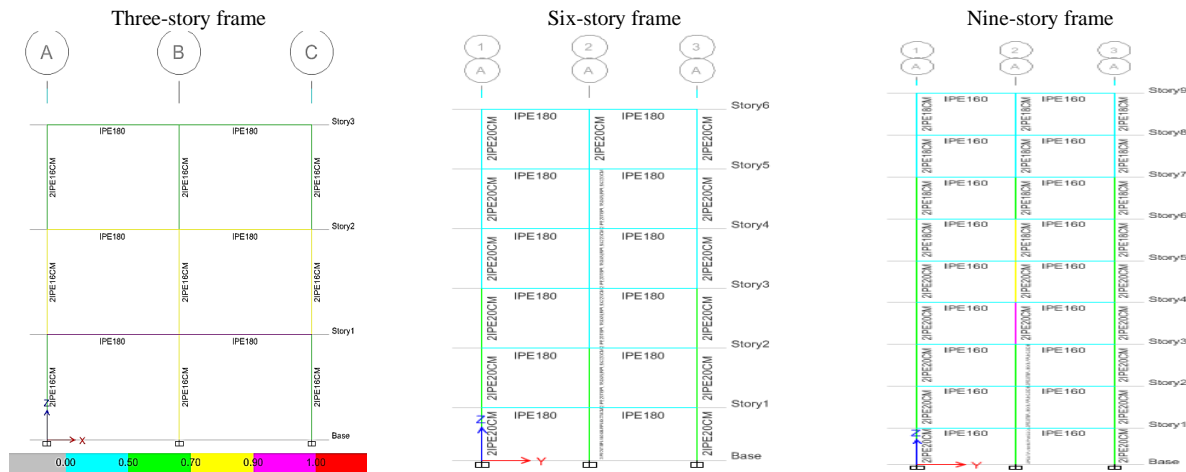


Figure 3. Diagonal, chevron, and toggle configurations of a viscous damper in the reference frame



**Figure 4.** Three-dimensional view of the reference frames with viscous damper (diagonal configuration)

considered in the current study, e.g. in the first state, the braces’ areas are  $1536 \text{ mm}^2$  for the two lower floors and  $1244 \text{ mm}^2$  for the two upper floors. To understand the effects of braces’ stiffness (braces’ area), the different areas for the braces have been used as indicated in Table 2. As indicated, 12 different states for braces’ area are considered in the current study, e.g. in the first state, the braces’ areas are  $1536 \text{ mm}^2$  for the half lower stories (in three-story building it is 1<sup>st</sup> story, in the six-story building



**Figure 5.** Three-dimensional view of reference frames with viscous damper (diagonal configuration)

**TABLE 1.** Frame elements properties in ANSYS simulations

Floors	Beams	columns	Braces
Three-story structure	IPB 18	2IPE16CM	
Six-story structure	IPB 18	2IPE20CM	Box 100×4
Nine-story structure	IPB 16	2IPE18CM 2IPE20CM	Box 90×3.6

they are 1<sup>st</sup> to 3<sup>rd</sup> stories, and in nine-story building, they are 1<sup>st</sup> to 5<sup>th</sup> stories) and  $1244 \text{ mm}^2$  for the two upper floors.

**3. 2. Finite Element Model** A finite element software, ANSYS, is employed to do numerical simulations in the current study. To develop the simulations by ANSYS, the element “Beam 188” whose functionality is similar to Timoshenko beam theory, has been allocated to the columns and beams. The elasticity modulus, Poisson’s ratio and density of Beam 188 are respectively  $E = 2 \times 10^{11}$ ,  $\nu = 0.3$  and  $\rho =$

$7800 \text{ kg/m}^3$ . The mentioned element can be used in linear or nonlinear analyses. To simulate the viscous damper, an element named “Combin14”, able to twist and do axial movements, has been exploited. The mass can be considered using a “Mass 21” element.

**4. RESULTS AND DISCUSSION**

**4. 1. Verification of Viscous Damper Simulations**

To verify the viscous damper simulations in ANSYS, a steel frame with three stories have been considered under the 1940 El-Centro earthquake excitation. Figure 6 indicates the experimental model of the mentioned structure in a 1/4 scale conducted by Constantinou and Symans [29]. The seismic response of this building has been investigated for 0.2.4 and 6 diagonal viscous dampers. The simulated models of the structure with these viscous dampers are illustrated in Figure 7. The total mass of the building is  $2900 \text{ kg}$  which has been distributed equally between the stories.

**TABLE 2.** Braces’ areas considered in this study for developing the simulations with ANSYS

State number		1	2	3	4	5	6	7	8	9	10	11	12
Area ( $\text{mm}^2$ )	Half lower stories	1536	1900	2256	2604	2944	3276	3600	3916	4224	4524	4816	5100
	Half upper stories	1244	1376	1700	2016	2324	2624	2916	3200	3476	3744	4004	4256

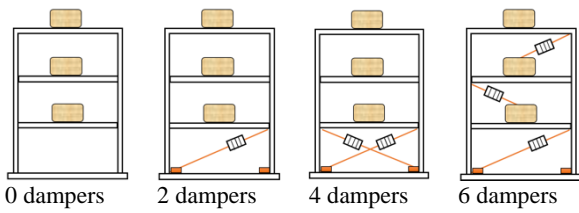


**Figure 6.** The experimental model of the three-story steel frame with various numbers of viscous dampers [29]

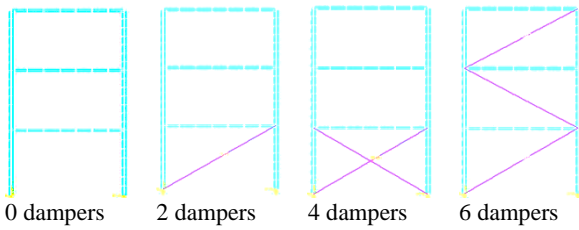


**Figure 7.** The ANSYS software simulated models of three-story steel frame with various viscous dampers

Table 3 illustrates the results of the experimental study conducted by Constantinou and Symans [29] and numerical simulations developed in this paper. As indicated, there is no considerable difference between the results of the experimental and numerical models, and so it can be concluded that the simulated damper performance is verified.

As indicated in Table 3, in the case of no viscous damper, experimental and numerical models behave strictly similar in simulating the stories displacement, in a way that their difference is less than 0.5%. However, in the case of damper existence, the experimental model results for stories displacement are more than those of the numerical model. In these cases, the minimum difference is 11.73%. The latter result can be attributed to either viscous damper modelling or the interaction between viscous damper and structure. In reality, the interaction between the damper and braces of the structure during the

vibration causes the axial displacement of the viscous damper to decrease and as a result of this, the resistant force of the damper will decrease. Moreover, in the experimental model, the behavior of the damper is considered linear, but this is not exactly correct in the field observations.

#### 4. 2. Damping Coefficient Effects on the Performance of Brace-viscous Damper System

In order to figure out the effects of damping coefficient on the performance of brace-viscous damper system (in terms of story displacement and story shear force), we developed some numerical simulations on the reference buildings using various values of damping coefficients. To do this, we considered diagonal configurations in all the buildings and the effects of damping coefficients variations are evaluated by the means of maximum story displacement and shear force of the stories. Figure 8 summarizes the effects of damping coefficient on the maximum displacements of the stories for the three-stories building. As indicated the maximum displacement of the stories reduces by increasing the damping coefficient. This reduction is more clear when  $C_D \leq 250 \text{ KNS/m}$ , but out of this range, the displacements marginally decrease with an increase in the damping coefficient. The latter trend can be attributed to the damper stiffness' increase against lateral forces. Hence, the largest  $C_D$  is not necessarily equal to the optimal damping coefficient. We investigated the optimal damping coefficients for various stories of the reference buildings in Section 4.5. The same trend is observed for six-story and nine-story buildings under the various earthquake records.

To investigate the dynamic response (in terms of maximum story displacement and base shear force) of the reference structures equipped with brace-viscous damper system (diagonal configuration) against various earthquake records, we numerically extracted the variation trend of maximum story displacements as

**TABLE 3.** The Constantinou and Symans [29] experimental and the current paper numerical results for the three-story steel frame

Earthquake 50% El Centro	Number of dampers	Peak base shear weight	Peak drift of the story height (%)
The Results of the experimental study [29]	0	0.295	1.498
	2	0.196	0.865
	4	0.159	0.660
	6	0.138	0.510
The results of the current paper by ANSYS	0	0.290	1.500
	2	0.179	0.775
	4	0.116	0.539
	6	0.105	0.477

well as maximum base shear at various stories under the action of the reference earthquake records. It should be noted that in all the cases  $C_D = 300 \text{ KNS/m}$  (Figure 9). As shown in Figure 9, the performance of the brace-viscous damper varies for various earthquake records since their dominant frequency is different. Regarding the reduction rate of maximum base shear, it is very low when  $C_D \geq 250 \text{ KNS/m}$  in comparison to that when  $C_D < 250 \text{ KNS/m}$ .

**4. 3. Configuration Effects on the Performance of Brace-viscous Damper System**

The damper configuration can affect the performance of a brace-viscous damper system in mitigation the structural dynamic response. In order to investigate the effects of brace-viscous damper configurations effects of the dynamic response of the reference buildings, a six-story steel building and Tabas earthquake are selected as the reference building and earthquake record, respectively. As indicated in Figure 10, the toggle configuration has the most control in structure response when the damping coefficient is in the range of  $0 \leq C_D \leq 500000 \text{ NS/m}$  and its performance is the worst when  $C_D > 500000 \text{ NS/m}$ . The latter finding is related to the large resistant forces produced by viscous damper due to its axial displacement magnification factor and also the interaction between the damper and brace.

Moreover, Figure 10 shows that the dynamic response mitigation associated with the chevron configuration is larger than that of diagonal configuration. This reduction is evident when  $0 \leq C_D \leq 500000 \text{ NS/m}$  for both the chevron and diagonal configurations. The structure response reduction is negligible for the damping coefficient more than  $500000 \text{ NS/m}$  and that's why the resistant force of the damper is more than the shear force of the stories. Moreover, for  $C_D \geq 500000 \text{ NS/m}$ , an increase in the damping coefficient will increase the resistant force of the damper, and so the interaction between the brace and viscous damper will be intensified, and as a result of this, the viscous damper adversely affects on the structure. The latter finding is evident from the values of structure displacements in the range of  $10^6 \leq C_D \leq 4 \times 10^6 \text{ NS/m}$  which goes high when the damping coefficient increases.

**4. 4. Brace Stiffness Effects on the Performance of Brace-viscous Damper System**

To figure out the variation trend of brace stiffness and dynamic response of structures, in this section the standard deviation of displacements of the 6<sup>th</sup> floor of a six-story building (reference building) against various values of braces' area (brace stiffness) is illustrated in Figure 11. In this figure the horizontal axis is referred to the state number of braces' area in Table 2, e.g. if state number is one, the

brace area in half lower stories is  $1536 \text{ mm}^2$  and in half upper stories is  $1244 \text{ mm}^2$ . As shown in Figure 11 the effects of the brace stiffness (changing the area of the braces) on the standard deviation of the displacements of the highest point of the structure.

As shown, by increasing the stiffness of the braces in a constant range, the interaction between the damper and the brace is reduced and the damper functionality improves in the reduction of the structure response. This reduction is seen until a specified value for the braces' area (e.g. for diagonal configuration, the state of brace area is 7; referring to Table 2 it reveals that the braces' area for half lower levels is  $3600 \text{ mm}^2$  and for half upper stories is  $2916 \text{ mm}^2$ ), but the structure response remains constant after these values. The latter issue is related to the fact that for braces area more than special values, the interaction between braces and damper wipe out and an increase in the braces' area will result in structure weight increase which adversely affects the structure response. Therefore, to have optimal designs, the brace area (stiffness) must be selected not more than determined values.

**4. 5. Optimizing the Brace-viscous Damper Arrangements for the Reference Building**

Based on sections (4.3) and (4.4), it has been shown that the toggle configuration outperforms the chevron and diagonal configuration in the mitigation of dynamic response of the reference buildings under the action of

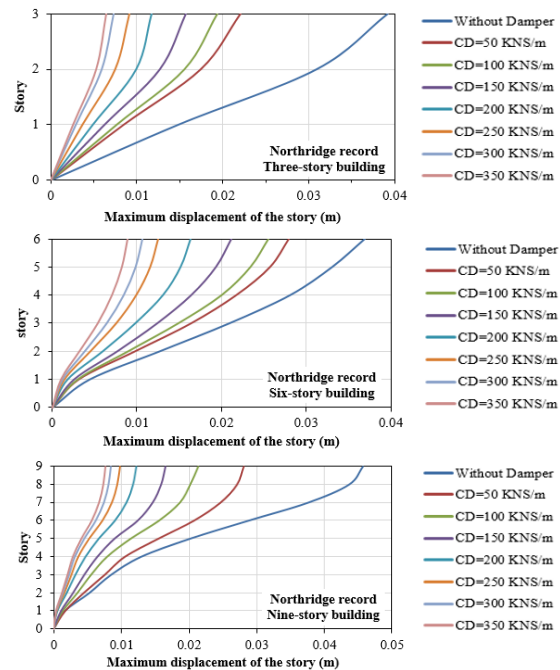


**Figure 8.** Maximum story displacements for various values of damping coefficients (in diagonal configuration) for a three-story building under various earthquake records

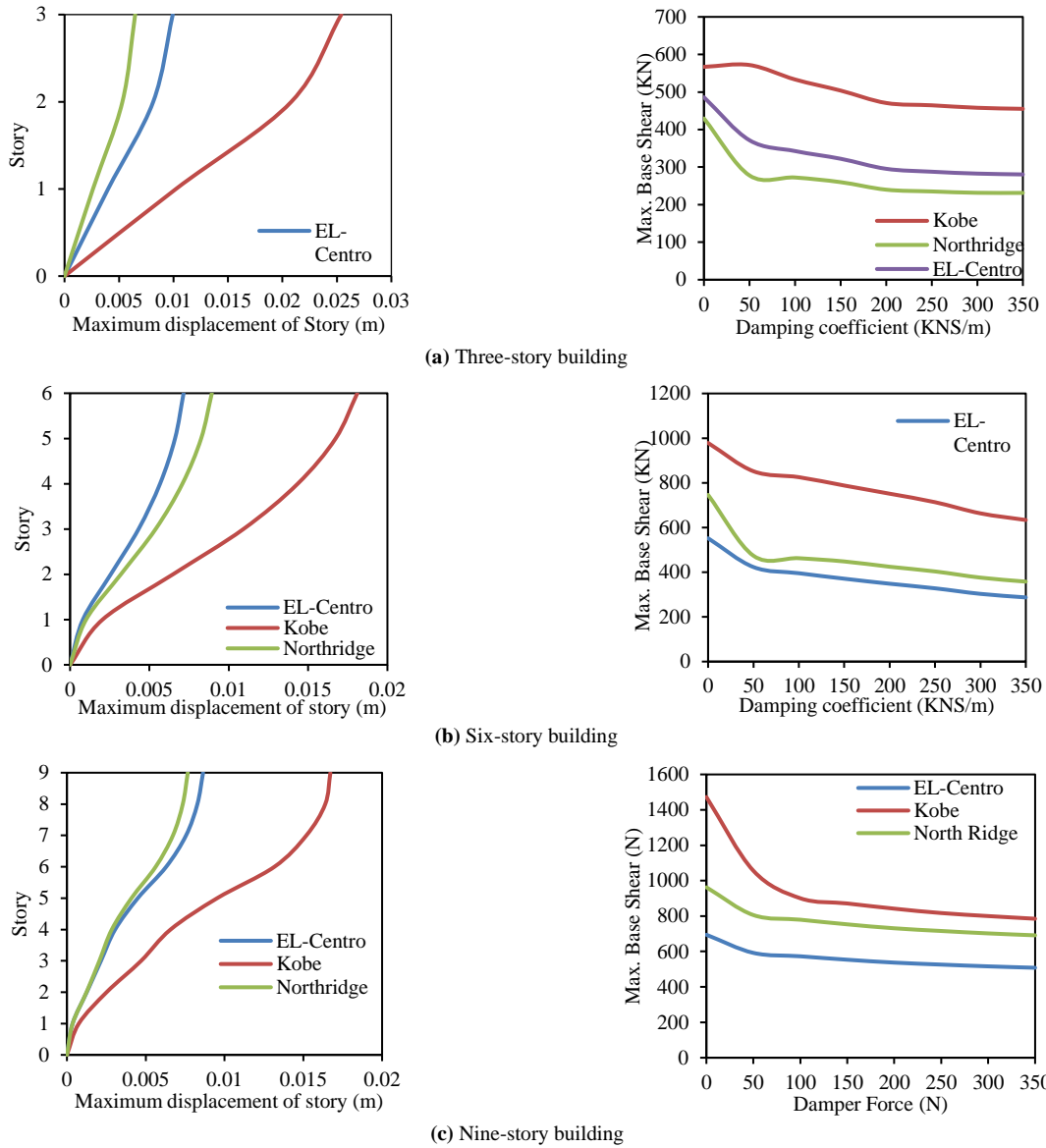


**Figure 9.** Maximum story displacements and base shear forces for different earthquake records for (a) three-story building, (b) six-story building, and (C) nine-story building

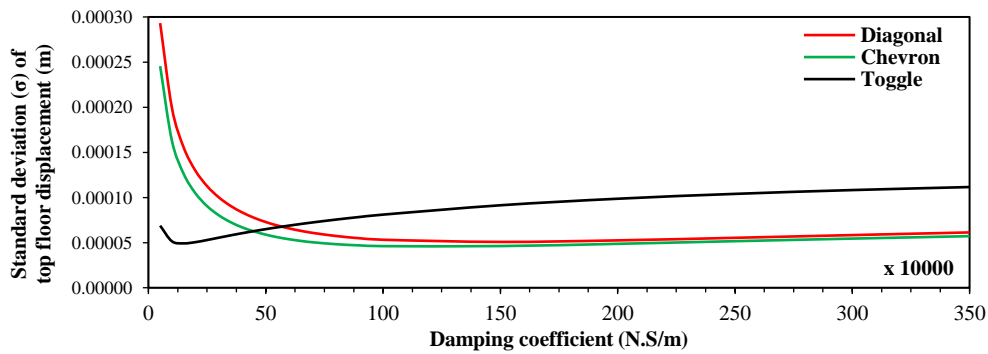


**Figure 10.** The standard deviation of displacement of the 6th story in the reference building (six-story building) against the damping coefficient

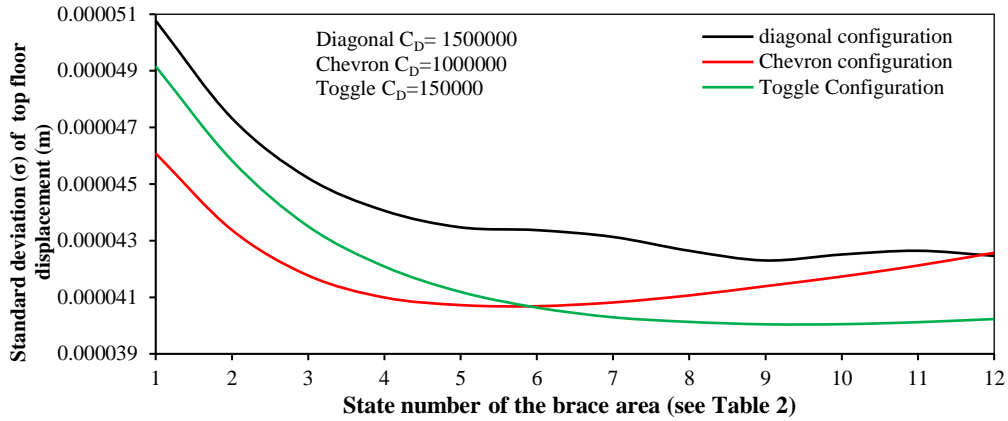


**Figure 11.** The standard deviation of the displacements of the 6th story in the reference building (six-story building) against the braces' area (mm<sup>2</sup>) with constant damping coefficient

Tabas earthquake. Hence, in this section, we are seeking to determine the most optimal arrangement of this configuration. To do this, the optimization process is devoted to the determination of most optimal damping coefficients at various stories of the three-story building under the Tabas Earthquake record. Table 4 summarizes the results of optimal arrangements for the toggle configuration in the reference steel frame. To do optimization, first, all the ranged from  $100 \times 10^3 - 500 \times 10^3 \text{ NS/m}$ . The values of  $\sigma$  (the standard deviations of the top point displacements) revealed that the most optimal damping coefficient for 4th story is  $100 \times 10^3 \text{ NS/m}$  which corresponds to the least

$\sigma=4.92 \text{ mm}$ . Afterwards, to determine the most optimal damping coefficients of 3rd story, the damping coefficient of 4th story assumed to be  $100 \times 10^3 \text{ NS/m}$  while this value was  $500 \times 10^3 \text{ NS/m}$  for the 1st and 2nd stories. The results of Table 4 indicate that increasing the damping coefficient up to  $300 \times 10^3 \text{ NS/m}$  will significantly reduce  $\sigma$ , but the standard deviation of displacements are almost constant for  $C_D > 300 \times 10^3 \text{ NS/m}$ . That's why we selected  $C_D = 300 \times 10^3 \text{ NS/m}$  as the most optimal damping coefficient of the third story. Similarly, the most optimal damping coefficients of first and second stories are determined.

**TABLE 4.** The displacement of the top point of the structure for non-uniform distribution of the viscous damper in toggle configuration for a brace area of 3916 mm<sup>2</sup> for two lower floors and 3200 mm<sup>2</sup> for two upper stories

Desired story*	damping coefficient (N.S/m)*10 <sup>3</sup>				The standard deviation of deck displacement (mm)* 10 <sup>-5</sup>
	Fourth story	Third story	Second story	First story	
Third story	<b>100</b>	500	500	500	4.92
	200	500	500	500	5.24
	300	500	500	500	5.95
	400	500	500	500	6.05
	500	500	500	500	6.49
Second story	100	100	500	500	5.21
	100	200	500	500	5.67
	100	<b>300</b>	500	500	5.99
	100	400	500	500	6.10
	100	500	500	500	6.24
First story	100	300	100	500	5.27
	100	300	200	500	5.60
	100	300	300	500	5.82
	100	300	<b>400</b>	500	6.13
	100	300	500	500	6.14

\*The story in where the optimal damping coefficient will be specified for it while the damping coefficients of the other stories are constant.

Damping coefficients were assumed to be  $500 \text{ NS/m}$ ; however, the damping coefficients of the 4th story.

## 5. SUMMARY AND CONCLUSIONS

In this paper, the effects of different configurations as well as braces' stiffness on the performance of brace-viscous damper systems implemented in various steel frame under different earthquake records have been studied. To do this, numerical simulations developed using a finite element software, ANSYS. To validate the performance of viscous damper in simulated models by ANSYS, the numerical results are verified against the experimental findings of Constantinou and Symans under the action of El-Cento earthquake. The results suggested that both the numerical and experimental models behave similarly.

The results of our simulations showed that regarding the displacement response of the top point of the structure, toggle configuration even with low damping coefficients outperforms the chevron and diagonal configurations. Further, comparing the structure displacements associated with the chevron and diagonal configurations indicated that the chevron configuration can better mitigate the dynamic response of the structure.

Regarding damping coefficient effects on the dynamic response of the structures, the maximum displacement of the stories reduces by increasing the damping coefficient. This reduction is more clear when  $C_D \leq 250 \text{ KNS/m}$ , but out of this range, the displacements marginally decrease with an increase in the damping coefficient. The latter trend can be attributed to the damper stiffness' increase against lateral forces.

The toggle configuration has the most control in structure response when the damping coefficient is in the range of  $0 \leq C_D \leq 500000 \text{ NS/m}$  and its performance is the worst when  $C_D > 500000 \text{ NS/m}$ . The dynamic response mitigation associated with the chevron configuration is larger than that of diagonal configuration. This reduction is evident when  $0 \leq C_D \leq 500000 \text{ NS/m}$  for both the chevron and diagonal configurations. The structure response reduction is negligible for the damping coefficient more than  $500000 \text{ NS/m}$  and that's why the resistant force of the damper is more than the shear force of the stories. Moreover, for  $C_D \geq 500000 \text{ NS/m}$ , an increase in the damping coefficient will increase the resistant force of the damper, and so the interaction between the brace and viscous damper will be intensified, and as a result of this, the viscous damper adversely affects on the structure. The latter finding is evident from the values of structure displacements in the range of  $10^6 \leq C_D \leq 4 \times$

$10^6 \text{ NS/m}$  which goes high when the damping coefficient increases.

Regarding the braces' stiffness, the results indicate that with an increase in braces' stiffness, the interaction between the viscous damper and the braces reduces, which would then be accompanied by increased damper performance and more control on the structure response. The results of this paper also are exploited to determine the optimized arrangement for braces and dampers. To do this, the variation of the standard deviations of structure displacements were compared for various damping coefficients. The most optimal damping coefficient corresponds to the value that significantly reduces the standard deviation of structure displacements.

## 6. REFERENCES

1. Cao, H., Reinhorn, A. M., and Soong, T. T., "Design of an Active Mass Damper for a Tall TV Tower in Nanjing, China." *Engineering Structures*, Vol. 20, No. 3, (1998), 134-143.
2. Chen, Y.T., Chai, Y.H., "Effects of brace stiffness on performance of structures with supplemental Maxwell model-based brace-damper systems." *Earthquake Engineering and Structural Dynamics*, Vol. 40, No. 1, (2011), 75-92.
3. Chopra, A.K., "Dynamics of Structures: Theory and Applications to Earthquake Engineering." Pearson, (1981).
4. Constantinou, M.C., and Symans, M.D., "Experimental and Analytical Investigation of Seismic Response of Structures with Supplemental Fluid Viscous Dampers." Buffalo, New York, (1992).
5. Constantinou, M.C., Panos T., Wilhelm H., and Sigaher A.N., "Toggle-Brace-Damper Seismic Energy Dissipations Systems." *Journal of Structural Engineering New York*, Vol. 127, No. 2, (2001), 105-112.
6. Di Sarno, L., Elnashai, A.S., "Bracing systems for seismic retrofitting of steel frames." *Journal of Constructional Steel Research*, Vol. 65, No. 2, (2009), 452-465.
7. Douglas P.T., "Toggle linkage seismic isolation structure." US5870863A, (issued 1996).
8. Elshafey, A.A., Haddara, M.R., and Marzouk, H., "Dynamic Response of Offshore Jacket Structures under Random Loads." *Marine Structures*, Vol. 22, No. 3, (2009), 504-521.
9. Federal Emergency Management Agency., "NEHRP Guidelines for The Rehabilitation." FEMA, (1997).
10. Fikri, J., Huang, L.J., "Passive Vibration Control Analysis of a Mosque Structure Using Diagonal Bracing Damper and Toggle Bracing Damper." In Proceedings of 4th IEEE International Conference on Applied System Innovation 2018, ICASI 2018, (2018).
11. Housner, G.W., Bergman, L.A., Caughey, T.K., Chassiakos, A.G., Claus, R.O., Masri, S.F., Skelton, R.E., Soong, T.T., Spencer, B.F., Yao, J.T.P., "Structural Control: Past, Present, and Future." *Journal of Engineering Mechanics*, Vol. 123, No. 9, (1997), 897-971.
12. Hwang, J.S., Huang, Y.N., Hung, Y.H., "Analytical and experimental study of toggle-brace-damper systems." *Journal of Structural Engineering*, Vol. 131, No. 7, (2005), 1035-1043.

13. Ibrion, M., Parsizadeh, F., Naeini, M.P., Mokhtari, M., Nadim, F., "Handling of dead people after two large earthquake disasters in Iran: Tabas 1978 and Bam 2003 – Survivors' perspectives, beliefs, funerary rituals, resilience and risk." *International Journal of Disaster Risk Reduction*, Vol. 11, (2015), 60-77.
14. Kandemir-Mazanoglu, E.C., Mazanoglu, K., "An optimization study for viscous dampers between adjacent buildings." *Mechanical Systems and Signal Processing*, Vol. 89, (2017), 88-96.
15. Kobori, Takuji, Koshika, N., Yamada, K., Ikeda, Y., "Seismic-response-controlled structure with active mass driver system. Part 1: Design." *Earthquake Engineering & Structural Dynamics*, Vol. 20, No. 2, (1991), 133-149.
16. Kobori, T., Koshika, N., Yamada, K., Ikeda, Y., "Seismic-response-controlled structure with active mass driver system. Part 2: Verification." *Engineering & Structural Dynamics*, Vol. 20, (1991), 151-166.
17. Lee, D., Taylor, D.P., "Viscous damper development and future trends." *Structural Design of Tall Buildings*, Vol. 10, No. 5, (2001), 311-320.
18. McNamara, R.J., Huang, C.D., Wan, V., "Viscous-damper with motion amplification device for high rise building applications." In: Structures Congress 2000: Advanced Technology in Structural Engineering, Philadelphia, Pennsylvania, United States, (2000).
19. Mehrabi, M.H., Suhatril, M., Ibrahim, Z., Ghodsi, S.S., Khatibi, H., "Modeling of a viscoelastic damper and its application in structural control." *Plos One*, Vol. 12, No. 6, (2017), e0176480.
20. Ou, J.P., Long, X., Li, Q.S., "Seismic response analysis of structures with velocity-dependent dampers." *Journal of Constructional Steel Research*, Vol. 63, No. 5, (2007), 628-638.
21. Patil, K.C., Jangid, R.S., "Passive control of offshore jacket platforms." *Ocean Engineering*, Vol. 32, No. 16, (2005), 1933-1949.
22. Soong, T.T., Dargush, G.F., "Passive Energy Dissipation Systems in Structural Engineering." Wiley, (1997).
23. Soong, T.T., Spencer, B.F., "Active Structural Control: Theory and Practice." *Journal of Engineering Mechanics*, Vol. 118, No. 6, (1992), 1282-1285.
24. Spencer, B.F., Sain, M.K., "Controlling buildings: A new frontier in feedback." *Shock and Vibration Digest*, Vol. 17, No. 6, (1997), 19-35.
25. Tabeshpour, M.R., Komachi, Y., "Rehabilitation of jacket offshore platforms using friction damper device and buckling restrained braces under extreme loads." In Proceedings of the Institution of Mechanical Engineers Part M: *Journal of Engineering for the Maritime Environment*, Vol. 233, No. 1 (2019), 209-217.
26. Türker, T., Bayraktar, A., "Experimental and numerical investigation of brace configuration effects on steel structures." *Journal of Constructional Steel Research*, Vol. 67, No. 5, (2011), 854-865.
27. Vaezi, M., Pourzangbar, A., Mamandi, S., Abdorrahman, S.O., "Seismic modeling of a buttress under Varzaqan earthquake record using ANSYS." Conference on Civil Engineering, Architecture, and Urbanism of the Islamic countries, Tabriz, Iran, (2018).
28. Vaezi, M., Pourzangbar, A., Fadavi, M., Rahbar Ranji, A., "Configuration effects of the performance of viscous dampers." 4th international congress on Civil Engineering, Architecture and Urban Development. Shahid Beheshti University, Tehran, Iran, (2016).
29. Vaezi, M., Pourzangbar, A., Mamandi, S., Abdorrahman, S.O., "Effects of configuration and brace stiffness on the performance of viscous dampers in steel frames." Conference on Civil Engineering, Architecture, and Urbanism of the Islamic Countries, Tabriz, Iran, (2018).
30. Yu, H., Gillot, F., Ichchou, M., "Reliability based robust design optimization for tuned mass damper in passive vibration control of deterministic/uncertain structures." *Journal of Sound and Vibration*, Vol. 332, No. 9, (2013), 2222-2238.
31. Zhang, B., He, L., Chen, G., Zhang, Z., Lv, C., "Experimental study on barrel viscous dampers and pipe hoops in pipeline vibration reduction." *High Technology Letters*, Vol. 20, (2014), 451-457.
32. Zhang, R., He, H., Weng, D., Zhou, H., Ding, S., "Theoretical analysis and experimental research on toggle-brace-damper system considering different installation modes." *Shock and Vibration Digest*, Vol. 19, No. 6, (2012), 1379-1390.

---

### Persian Abstract

#### چکیده

بارهای دینامیکی مانند زلزله باعث ارتعاش سازه در مودهای مختلف می شوند. دامنه این ارتعاشات به شدت به بارهای دینامیکی اعمال شده بستگی دارد. سیستم کاهنده انرژی مانند سیستم مهاربند- میراگر ویسکوز می تواند با تولید نیروی مقاوم بخشی از ارتعاشات سازه را کاهش دهند. حداکثر کارایی سیستم مهاربند- میراگر ویسکوز زمانی حاصل خواهد شد که نیروی مقاومی تولید شده توسط این سیستم حداکثر مقدار خود را داشته باشد. بر این اساس، پیکربندی میراگر ویسکوز، همچنین سختی مهاربند می تواند به طور چشمگیری عملکرد سیستم مهاربند- میراگر ویسکوز را بهبود دهد. در این مقاله، تاثیر سه نوع پیکربندی میراگر ویسکوز (شامل پیکربندی زانویی، قطری و چورن) و نیز تاثیر سختی مهاربند بر عملکرد سیستم مهاربند- میراگر ویسکوز در یک سازه فولادی ۸ طبقه تحت بار زلزله طیس بررسی شده است. برای مدل سازی از نرم افزار المان محدود انسیس استفاده شده است. نتایج مدل سازی های عددی با استفاده از مطالعات آزمایشگاهی موجود در مقاله صحت سنجی شده اند. نتایج نشان می دهند که پیکربندی زانویی نیروی برشی پایه را نسبت به نسبت پیکربندی های چورن و قطری بیشتر کاهش می دهد. همچنین، افزایش سختی مهاربند باعث کاهش اندرکنش بین مهاربند و میراگر شده و در نتیجه عملکرد سیستم مهاربند- میراگر ویسکوز را بهبود می بخشد. نهایتاً چیدمان بهینه سازی شده برای سیستم مهاربند- میراگر ویسکوز برای ساختمان مورد مطالعه ارائه شده است.

---